International Journal of Engineering & Scientific Research (IJMRA Publications)
Vol. 6 Issue 6, June 2018,
ISSN: 2347-6532 Impact Factor: 6.660
Journal Homepage: http://www.esrjournal.com Email: esrjeditor@gmail.com
Double-Blind Peer Reviewed Refereed Open Access International Journal - Included in the International Serial Directories Indexed & Listed at: Ulrich's Periodicals Directory ©, U.S.A., Open J-Gage as well as in Cabell's Directories of Publishing Opportunities, U.S.A

Corrosion inhibition performance of dithiocarbamate based inhibitors for mild steel in acidic medium: electrochemical, theoretical and surface analysis studies.

Arun Lal,[a,c,*], Raj Kishore Sharma,[c] Gurmeet Kaur[b,c], Gurmeet Singh[c*]

[a]Department of Chemistry, Rajdhani College, NewDelhi-10015,

[b]Department of Chemistry, SGTB Khalsa College, Delhi-110007.

[c]Department of Chemistry, University of Delhi, Delhi -110007

Abstract:

The present work has been reported with the synthesis of two dithiocarbamate inhibitors namely sodium (2E,2'E)-2,2'-(ethane-1,2-diylidene)bis(hydrazinecarbodithioate) (En-DTC) and sodium (((1E,1'E)-ethane-1,2-diylidenebis(azanylylidene))bis(ethane-2,1diyl))dicarbamodithioate (Hy-DTC) and their corrosion inhibition behavior for mild steel in 0.5 M H_2SO_4 solution using electrochemical studies. We observed that En-DTC and Hy-DTC are efficient inhibitors showing maximum inhibition efficiency as 97% and 98%, respectively at 298 K. The potentiodynamic studies showed that both compounds were mixed-type of inhibitor. Both the inhibitors follow Langmuir adsorption model with negative value of free energy of adsorption (ΔG^0_{ads}) and negative value of ΔG^0_{ads} indicate towards the spontaneity of the adsorption process. Quantum chemical studies were performed on the inhibitor molecules which configured the favorable correlation between molecular structure of inhibitor and their inhibition property. Scanning electron microscopy (SEM) and atomic force microscopy (AFM) were used to study the surface morphology of the mild steel samples.

*Corresponding authors.

E-mail addresses: gurmeet123@yahoo.com (G. Singh). arunlal035@gmail.com (Arun Lal)

1. Introduction

Iron and its alloys have special properties like mechanical strength and high structural strength, owing to these properties they are excessively used in various applications like gas, oil, pharmaceutical and chemical industries. [1,2]. Metal surfaces are cleaned by acid-pickling, acid-descaling, acid-cleaning and oil-well acidizing using acid solutions in these industrial processes. However, acid reacts with metal, which leads to corrosion resulting in severe destruction to metal and increasing maintenance cost to industry [3–8]. The most common corrosion inhibition method involves selection of proper material and cathodic protection. But, these methods are cumbersome, costly in nature and unpractical for wider industrial application. So, there is always a need to find a low cost and environment friendly method to prevent corrosion of metals. Due to their low cost and ease of handling, the organic molecules have emerged as promising corrosion inhibitors for corrosion caused by acid attack on metals. The organic molecules containing hetero atoms adsorb strongly on the metal surface and provide an effective barrier preventing occurrence of corrosion reaction at solution-metal interface [9–21]. The dithiocarbamate (DTC) compound contains two sulfur atoms and one nitrogen atom and are known to chelate strongly with metal surface [22]. Qafsaoui et.al reported use of 1-pyrrolidine dithiocarbamate as an environment friendly inhibitor to prevent corrosion on copper with high efficiency[23]. In its other report, Qafsaoui et.al used ammonium pyrrolidine dithiocarbamate as an inhibitor for corrosion on copper. They showed that ammonium pyrrolidine dithiocarbamate gets adsorbed rapidly on the copper surface and it works as a mixed inhibitor [24]. Qafsaoui et.al also reported the effective inhibition of corrosion by 1-pyrrolidine dithiocarbamate for AA2024-T_3 alloy [25]. Kicir et.al stated the use of ammonium(2,4-dimethylphenyl)-dithiocarbamate as an inhibitor for mild steel. They reported the inhibitor to hold an efficiency of 98% at concentration of 500 ppm solution [26]. In a different investigation, Zhang et.al reported the inhibiting behavior of ammonium pyrrolidine dithiocarbamate on copper surface with maximum inhibition efficiency of 98.7% in NaCl solution [27]. M.M.Singh et.al reported in their observation about the corrosion mitigation ability of piperidine dithiocarbamate on copper and its behavior as mixed type inhibitor [28]. Li et.al studied corrosion mitigation effect of sodium diethyldithiocarbamate on cold rolled steel. Their data showed that the inhibitor experiences both type of adsorption on metal surface i.e. physisorption and chemisorption, moreover sodium diethyldithiocarbamate follows Langmuir adsorption isotherm [29]. Encouraged by these reports, we studied the inhibition efficiency of two dithiocarbamate compounds namely two dithiocarbamate inhibitors

namely sodium (2E,2'E)-2,2'-(ethane-1,2-diylidene)bis(hydrazinecarbodithioate) (En-DTC) and sodium (((1E,1'E)-ethane-1,2-diylidenebis(azanylylidene))bis(ethane-2,1diyl))dicarbamodithioate (Hy-DTC). They were examined as corrosion inhibitors in 0.5 M H_2SO_4 solution for mild steel using electrochemical, theoretical and surface analysis. We also studied the thermodynamic feasibility and adsorption behavior of these inhibitors on mild steel.

2. Experimental method

Mild steel strips having cross section of 1 cm × 1 cm were used for the studies and had the following composition as determined by EDX spectra analysis C = 0.15, S = 0.02, Mn = 1.02, Si = 0.08 and Fe = 98.72. Before measurements, emery sheets of various grades (grade 100 to 2000) were used to polish the sample surfaces and samples were degreased using acetone, washed with double distilled H_2O and eventually dried in a vacuum desiccator. The electrochemical workstation (CHI 760D, CH Instruments, USA) was employed to conduct all electrochemical studies. The studies were performed with concentrations 10^{-2} M, 10^{-3} M, 10^{-4} M and 10^{-5} M at four temperatures i.e. 298 K, 308 K, 318 K and 328 K. In the operating three electrode assembly system, working electrode comprised of low-carbon steel sample with $1cm^2$ of the open area, platinum electrode acted as auxiliary and a saturated calomel electrode (SCE) was used as reference electrodes. The (EIS) impedance measurements were studied at corrosion potential using frequency range 1Hz – 1kHz with amplitude 0.005 V. The grinded low carbon steel specimens were immersed within the blank (0.5 M H_2SO_4) and also in the solution containing the inhibitor DTCs for 4 hours. After that specimens were taken out, washed using distilled water, kept sometime to dry and were studied under a scanning electron microscope (model SEM-JSM-6610 LV). The AFM study of low-carbon steel samples with and without inhibitors were obtained using a Nanosurf Naio AFM instrument. Quantum chemical calculations for inhibitors were determined using Austin Method 1 (AM1). The Hypercam 8.0 package program was used to determine molecular parameters.

3. Results and Discussion

Synthesis of Dithiocarbamates:-

Dithiocarbamate (a) sodium (2E,2'E)-2,2'-(ethane-1,2-diylidene)bis(hydrazinecarbodithioate) (En-DTC) and (b) sodium (((1E,1'E)-ethane-1,2-

diylidenebis(azanylylidene))bis(ethane-2,1diyl))dicarbamodithioate (Hy-DTC) were prepared from the procedure reported in literature (Fig.1)[30].

Polarization studies

The inhibition efficiency of En-DTC and Hy-DTC for mild steel in 0.5 M sulphuric acid solution were studied and the obtained cathodic and anodic polarization curves are shown in Fig.2 and Fig.3 respectively. Table 1 and Table 2 summarizes value of the electrochemical parameters of these polarization curves. With change in inhibitor concentration, Tafel slope of anodic and cathodic reaction change, which indicate that inhibitors are affecting both the reactions [31]. Generally, a change in value of E_{corr} more than 85 mV is considered as a parameter of classification for inhibitor to be anodic or cathodic type. En-DTC showed maximum shift of 21mV and Hy-DTC showed maximum shift of 31 mV at 298 K (Table 1 and 2), which indicates that En-DTC and Hy-DTC could behave as mixed-type inhibtors. This also points out that inhibitor molecules adsorbed on metal surface without much altering cathodic and anodic reaction mechanisms [32]. Inhibition efficiency (I.E.) increased significantly as I_{corr} decreased in presence of inhibitor En-DTC and Hy-DTC concentrations as compared to uninhibited solution, suggesting that inhibitors were working capably. A lot of variety of inhibitor molecules were absorbed per unit area on mild steel surface and thereby enhanced the inhibition efficiency with increased concentration of inhibitors. With rise in temperature, corrosion current increases and I.E. decreases for a particular concentration of inhibitor because of the increased rate of reaction at elevated temperatures and desorption of inhibitors from the metal surface [33,34].

Impedance studies

Nyquist plot and bode plots of solutions with varied concentration of En-DTC and Hy-DTC in 0.5 M H_2SO_4 solution are given in Fig.4 and Fig.5 respectively. The Nyquist plot shows change in the resistance response of mild steel in corrosive solutions upon addition of the inhibitor molecule. A single depressed capacitive loop in the impedance spectrum was obtained, which increases with the addition of inhibitor and is controlled by the charge transfer. the impedance loop don't seem to be a perfect semicircle because of dispersing effect, which can be attributed to the roughness of the surface, irregularity of electrode surfaces and inhibitors adsorption. The bodes plot show that with increase in inhibitor concentration within the solutions leads to additional negative values of the point at high frequencies, indicating larger inhibition ability of inhibitors at higher concentrations [35].

R_{ct} values of inhibited substrates area increase with the concentration of inhibitors as shown in Table 3. An increased charge transfer resistance indicates towards the additional slowly corroding system. However, the values of C_{dl} are reduced with increase in En-DTC and Hy-DTC concentration. This can be attributed to decrease in local dielectric constant and increase in the thickness of electrical double layer, indicating that inhibitors act through adsorption at metal/solution interface [36].

Effect of temperature

The plot of C_{inh} / θ vs C_{inh} for both En-DTC and Hy-DTC are straight line getting slope nearly equal to 1.00 and the best suitable adsorption model to fit in are obtained with Langmuir adsorption isotherm shown in Fig. 6 and Fig. 7 [37].

The ΔG^0_{ads} value of En-DTC and Hy-DTC in the acidic medium at four optimum temperatures are nearly -40 kJ/mol, indicating chemisorption process predominates and is spontaneous in nature Table 4 [38,39]. The negative value of ΔH^0_{ads} for all concentrations of dithiocarbamates shown in Table 4 is pointing that the adsorption of inhibitors on low-carbon steel is an exothermic process. The ΔH^0_{ads} , being higher than -40 kJ/mol also governs that inhibitor molecules were adsorbed by chemisorption process [40]. Similarly, negative value of ΔS^0_{ads} shows decrease in entropy or randomness during adsorption, favoring the orderly arrangement of inhibitor molecules on metal surface [41]. The corrosion current (Log I_{corr}) for both inhibitors were plotted against 1/T and presented in Fig. 8 and Fig. 9. The kinetic parameters (activation energy) were evaluated with and without inhibitor and are shown in Table 5 and Table 6. Activation energy of inhibitors were calculated using the following expression:

$$Log\ I_{corr} = \frac{-E_a}{2.303\ RT} + \mathbf{Log}\ A$$

The values of E_{act} (shown in Table 5 and Table 6) with the inhibitors were found out to be higher than in absence of inhibitors, indicating reduction in corrosion rate due to presence of an additional inhibitor protective barrier.

Surface characterization

Surface analysis (SEM) has been performed by using En-DTC and Hy-DTC as corrosion inhibitor additives with concentration 10^{-5} M and 10^{-2} M in 0.5 M H_2SO_4 solution on low-carbon steel sample and the results obtained are shown in Fig. 10. The presence of En-

DTC and Hy-DTC has controlled the corrosion to a larger extent. It was observed that the higher concentration of En-DTC and Hy-DTC leads to better corrosion protection. The mitigation action of inhibitor indicates towards protective covering formation on mild steel surface by adsorption of inhibitor molecules. The AFM images of mild steel dipped in 0.5 M H_2SO_4 solution with and without 10^{-5} M and 10^{-2} M concentration of En-DTC and Hy-DTC are shown in Fig. 11. As seen in images that the low-carbon steel surface dipped in 0.5 M H_2SO_4 containing 10^{-5} M and 10^{-2} M inhibitor appear smooth and less damaged than the steel surface immersed into acid solution alone. Moreover, the values of area roughness with the addition of 10^{-5} M and 10^{-2} M En-DTC was reduced to 733.9 nm and 465.7 nm respectively while the surface roughness for Hy-DTC was 628.1 nm and 315.9 nm at its lower and higher concentrations respectively.

This indicates inhibition ability at higher concentration of both inhibitors are high due to stronger film formation over mild steel surface [42].

Theoretical Studies

In Fig. 12 and Fig. 13, we observed that there is the formation of a transition state due to the interaction between frontier orbitals (HOMO and LUMO) of inhibitors. Larger values of E_{HOMO} for En-DTC (-8.84 eV) and Hy-DTC (-9.26 eV) are possible to specify a tendency of the molecule with low energy as shown in Table 7 and empty molecular orbital and facilitating surface assimilation by influencing the transport process through the adsorbed layer [43,44]. The lower absolute values of energy band gap (ΔE) for En-DTC (8.25 eV) and Hy-DTC (6.83 eV) offers better mitigation efficiencies, as a result, the energy to separate the last occupied orbital electron will be very low. Dipole moment value for En-DTC and Hy-DTC were 1.7 and 1.8 respectively which point towards the extent of polarization and increased electron donating ability to metal.

Conclusions:

The dithiocarbamate inhibitors namely sodium (2E,2'E)-2,2'-(ethane-1,2-diylidene)bis(hydrazinecarbodithioate) (En-DTC) and sodium (((1E,1'E)-ethane-1,2-diylidenebis(azanylylidene))bis(ethane-2,1diyl))dicarbamodithioate (Hy-DTC) were synthesized and the inhibition behavior of these compounds for mild steel in 0.5 M H_2SO_4 solution was studied. The polarization study indicates that both compounds are mixed type inhibitors. En-DTC and Hy-DTC are efficient inhibitors showing maximum inhibition efficiency as 97% and 98%, respectively at 298 K. The adsorption studied of the two

inhibitors follow Langmuir adsorption model. The results obtained from surface characterization are supporting the results of electrochemical and non-electrochemical studies.

Reference:-

[1] Jawich M.W.S , Oweimreen G.A , Ali S.A 2012 *Corros. Sci.* **65** 104–112.
[2] Daoud D , Douadi T, Issaadi S, Chafaa S 2014 Corros. Sci. **79** 50–58.
[3] Ramya K, Mohan R, Anupama K K, Joseph A 2015 *Mater. Chem. Phys.* **149** 632.
[4] Kumar C B P, Mohana K N 2014 *J. Taiwan Inst. Chem. Eng.* **45** 1031.
[5] Zhang S T, Tao Z H, Li W H , Hou B R 2009 *Appl. Surf. Sci.* **255** 6757.
[6] Shukla S K, Singh A K, Ahamad I, Quraishi M A, 2009 *Mater. Lett.* **63** 819.
[7] Saliyan V R, Adhikari AV 2008 *Corros. Sci.* **50** 55
[8] Mistry B M, Patel N S, Sahoo S, Jauhari S 2012 *Bull. Mater. Sci.* **35** 459.
[9] Chetouani A, Hammouti B, Benhadda T, Daoudi M 2005 *Appl. Surf. Sci.* **249** 375..
[10] Al Hamzi A H, Zarrok H, Zarrouk A, Salghi R, Hammouti B, Al-Deyab S S, Bouachrine M, Amine A, Guenoun F 2013 *Int. J. Electrochem. Sci.* **8** 2586.
[11] Vogt M R, Nichols R J, Magnussen O M, Behm R J 1998 *J. Phys. Chem. B* **102** 5859.
[12] Yildirim A,*Çetin* M 2008 *Corros. Sci*. **50** 155.
[13] Badawy W A, Ismail K M, Fathi A M 2006 *Electrochim. Acta* **51** 4182.
[14] Goulart C M, Esteves-Souza A, Martinez-Huitle C A, Rodrigues C J F, Maciel M A M, Echevarria A 2013 *Corros. Sci.* **67** 281.
[15] Sadeghi Meresht E, Shahrabi Farahani T, Neshati J 2012 *Corros. Sci*. **54** 36.
[16] Palomar-Pardavé M, Romero-Romo M, Herrera-Hernández H, Abreu-Quijano M A, Likhanova N V, Uruchurtu J, Juárez-García J M 2012 *Corros. Sci.* **54** 231.
[17] Hegazy M A, El-Tabei A S, Bedair A H, Sadeq M A 2012 *Corros. Sci.* **54** 219.
[18] Hosseini S M A, Azimi V 2009 *Corros. Sci.* **51** 728.
[19] Li X, Deng S, Fu H 2011 *Corros. Sci.* **53** 3241.
[20] Nataraja S E, Venkatesha T V, Manjunatha K, Poojary B, Pavithra M K, Tandon H C 2011 *Corros. Sci.* **53** 2651.
[21] Sheng X, Ting Y P, Pehkonen S O 2007 *Ind. Eng. Chem. Res.* **46** 7117.
[22] Shu X, Dang Z, Zhang Q, Yi X, Lu G, Guo C, Yang C 2013 *Miner. Eng.* **42** 36.
[23] Qafsaoui W, Kendig M W, Perrot H, Takenouti H, 2013 *Electrochim. Acta* **87** 348.
[24] Qafsaoui W, Kendig M W, Joiret S, Perrot H, Takenouti H 2016 *Corros. Sci.* **106** 96.
[25] Qafsaoui W, Kendig M W, Perrot H, Takenouti H 2015 *Corros. Sci*. **92** 245.
[26] Kicir N, Tansuğ G, Erbil M, Tüken T 2016 *Corros. Sci.* **105** 88.
[27] Zhang X H, Liao Q Q, Nie K B, Zhao L L, Yang D, Yue Z W, Ge H H, Li Y J 2015 *Corros. Sci.* **93** 201.
[28] Singh M M, Rastogi R B, Upadhyay B N 1994 *Corros. Sci.* **50** 620.
[29] Li L, Qu Q, Bai W, Yang F, Chen Y, Zhang S, Ding Z 2012 *Corros. Sci.* **59** 249.
[30] Gaur J, Jain S, Bhatia R, Lal A, Kaushik N K 2013 *J. Therm. Anal. Calorim.* **112** 1137.
[31] Quraishi M A, Sharma H K 2002 *Mater. Chem. Phys.* **78** 18
[32] Zhang G, Chen C, Lu M, Chai C, Wu Y 2007 *Mater. Chem. Phys.* **105** 331.
[33] Ramanavicius A, Finkelsteinas A, Cesiulis H, Ramanaviciene A 2010 *Bioelectrochemistry* **79** 11.
[34] Ferreira E S, Giacomelli C, Giacomelli F C, Spinelli A 2004 *Mater. Chem. Phys.* **83** 129.
[35] Karthikaiselvi R, Subhashini S, Rajalakshmi R 2012 *Arab. J. Chem.* **5** 517.
[36] Garcia S J, Markley T A, Mol J M C, Hughes A E 2013 *Corros. Sci.* **69** 346.
[37] Döner A, Şahin E A, Kardaş G, Serindağ O 2013 *Corros. Sci.* **66** 278.

[38] Tawfik S M 2016 *J. Mol. Liq.* **216** 624.
[39] Noor E A, Moubaraki A H A 2008 *Mater. Chem. Phys.* **110** 145.
[40] Kumar A, Trivedi M, Bhaskaran, Sharma R. Kishore, Singh G 2017 *New J. Chem.* **41** 8459.
[41] Zhang Q B, Hua Y X 2009 *Electrochim. Acta* **54** 1881.
[42] Singh P, Srivastava V, Quraishi M A 2016 *J. Mol. Liq.* **216** 164.
[43] Yadav M, Behera D, Kumar S, Sinha R R, 2013 *Ind. Eng. Chem. Res.* **52** 6318.
[44] Tan B, Zhang S, Qiang Y, Feng L, Liao C, Xu Y, Chen S, 2017 *J. Mol. Liq.* **248**, 902.

Caption of Figures

Fig. 1. Synthesis scheme for the preparation of En-DTC and Hy-DTC

Fig.2. Galvanostatic polarization curves for mild steel in 0.5 M H_2SO_4 containing different concentrations of (En-DTC) at various temperatures

Fig.3. Galvanostatic polarization curves for mild steel in 0.5 M H_2SO_4 containing different concentrations of (Hy-DTC) at various temperatures.

Fig.4. Bodes and Nyqst curves for mild steel in 0.5 M H_2SO_4 containing different concentrations of (En-DTC) at various temperatures

Fig.5. Bodes and Nyqst curves for mild steel in 0.5 M H_2SO_4 containing different concentrations of (Hy-DTC) at various temperatures.

Fig.6. Adsorption behavior of (En-DTC) on the mild steel surface in 0.5 M H_2SO_4.

Fig.7. Adsorption behavior of (Hy-DTC) on the mild steel surface in 0.5 M H_2SO_4.

Fig.8. Plot of variation of Log I_{corr} vs 1/T for different concentrations of (En-DTC).

Fig.9. Plot of variation of Log I_{corr} vs 1/T for different concentration of (Hy-DTC).

Fig.10. SEM images of surface of mild steel after immersion for 6 hrs in (b) 0.5 M H_2SO_4 and in the presence of (c) 10^{-2} M (d) 10^{-5} M En-DTC (e) 10^{-2} M (f) 10^{-5} M Hy-DTC [Magnification = 5000] at 298 K.

Fig.11. AFM Three-dimensional images of mild steel surfaces for (a) Mild Steel (b) 0.5 M H_2SO_4 (c) 10^{-2} M En-DTC (d) 10^{-5} M En-DTC (e) 10^{-2} M Hy-DTC (f) 10^{-5} M Hy-DTC

Fig.12. (a) Structure of En-DTC with Charge on Atoms (b) Molecular Orbital Plot for Total Charge Density (c) The Frontier Molecular Orbital Charge Density Distribution for HOMO and (d) The Frontier Molecular Orbital Charge Density Distribution for LUMO.

Fig.13. (a) Structure of Hy-DTC with Charge on Atoms (b) Molecular Orbital Plot for Total Charge Density (c) The Frontier Molecular Orbital Charge Density Distribution for HOMO and (d) The Frontier Molecular Orbital Charge Density Distribution for LUMO

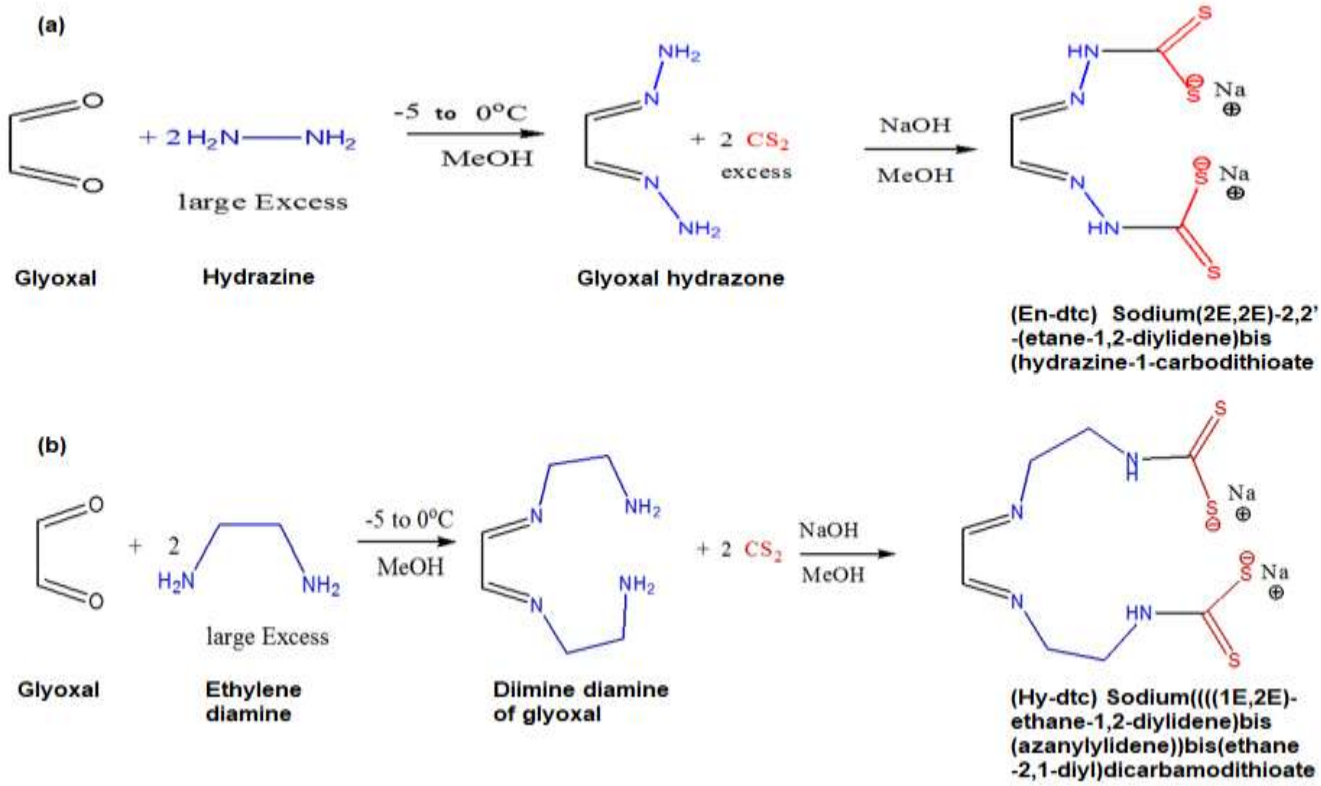

Fig. 1. A synthesis scheme of En-DTC and Hy-DTC

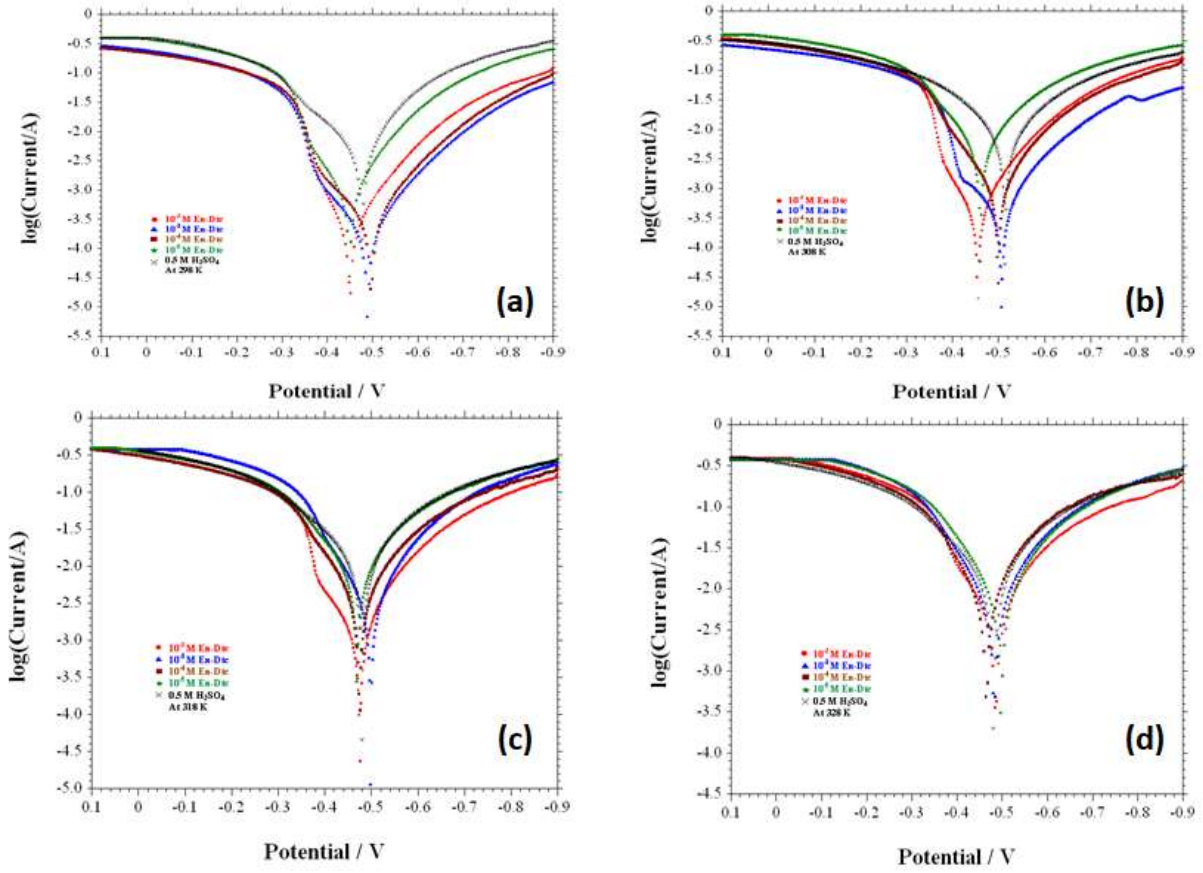

Fig.2. Galvanostatic polarization curves for mild steel in 0.5 M H_2SO_4 containing different concentrations of (En-DTC) at various temperatures.

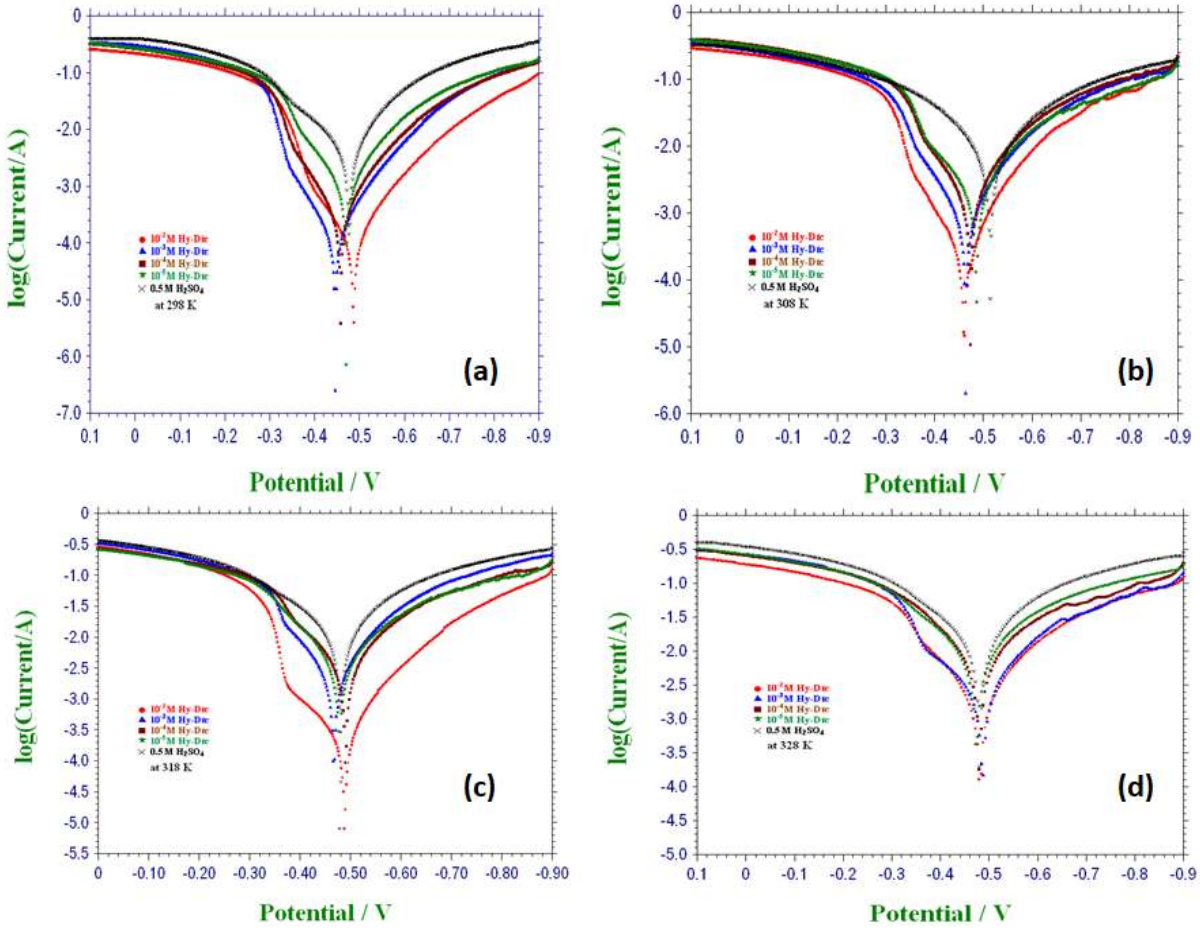

Fig.3. Galvanostatic polarization curves for mild steel in 0.5 M H_2SO_4 containing different concentrations of (Hy-DTC) at various temperatures.

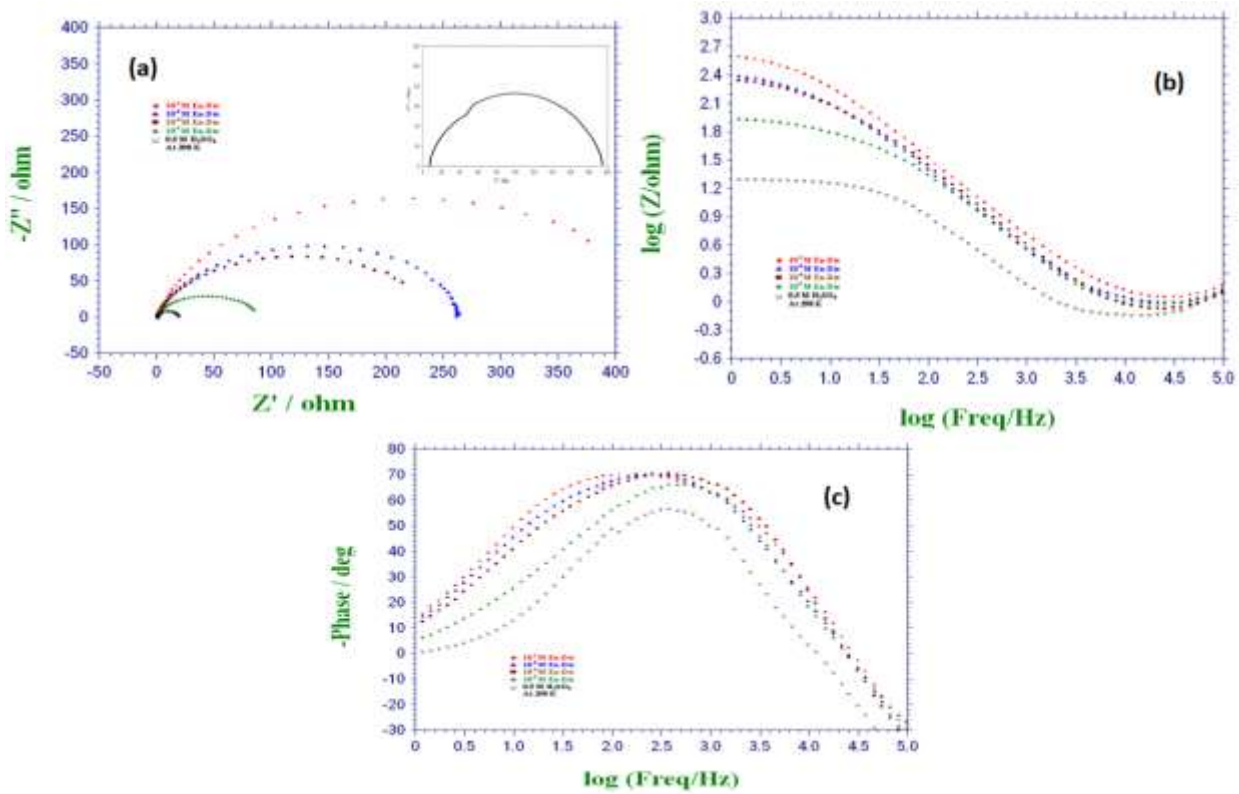

Fig.4. Bodes and Nyqst curves for mild steel in 0.5 M H_2SO_4 containing different concentrations of (En-DTC) at various temperatures.

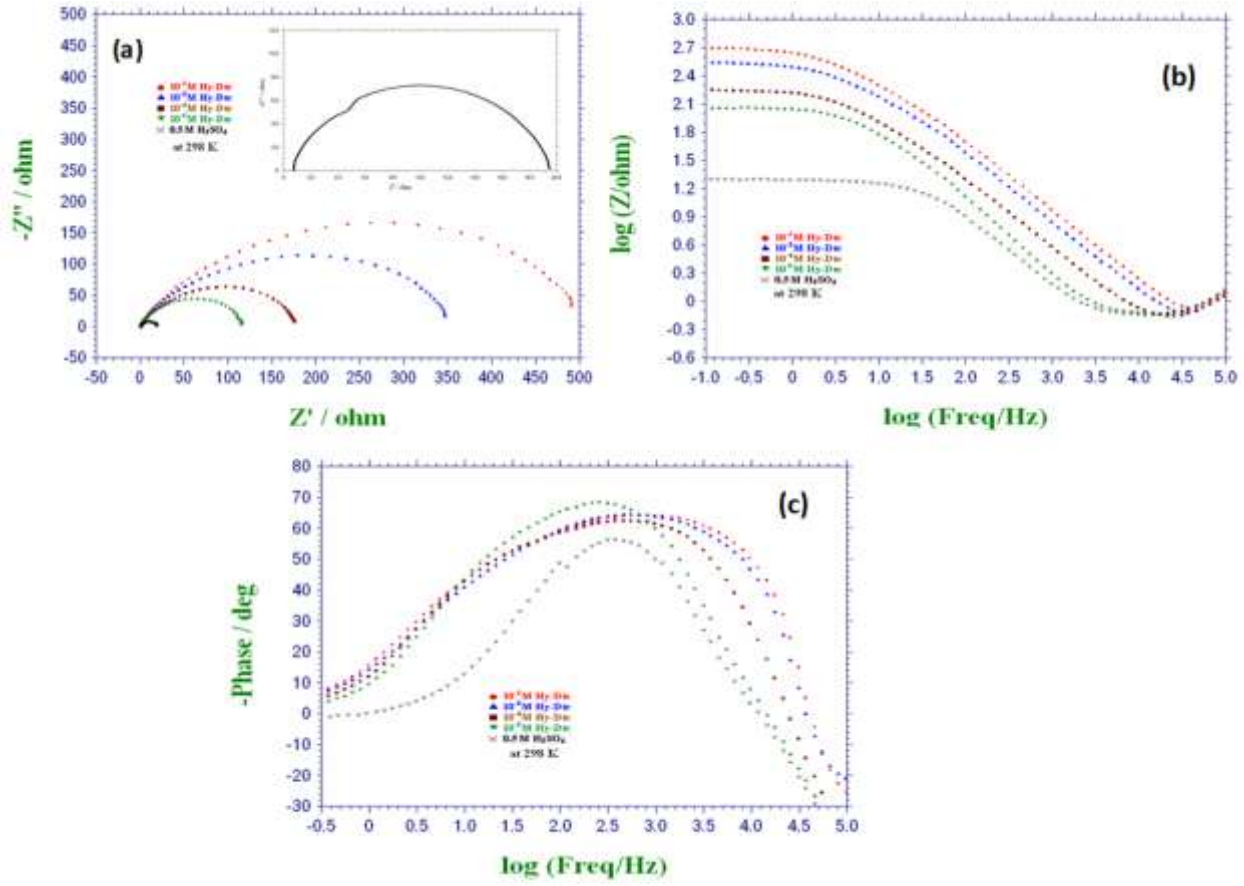

Fig.5. Bodes and Nyqst curves for mild steel in 0.5 M H_2SO_4 containing different concentrations of (Hy-DTC) at various temperatures.

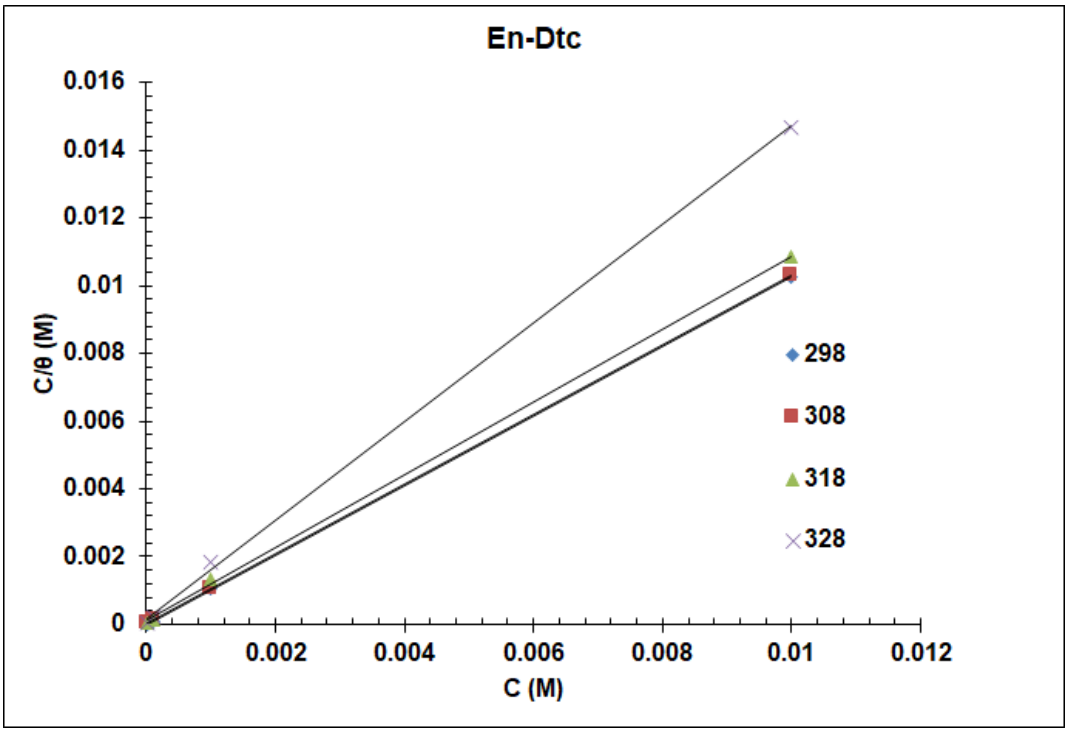

Fig.6. Adsorption behavior of (En-DTC) on the mild steel surface in 0.5 M H_2SO_4.

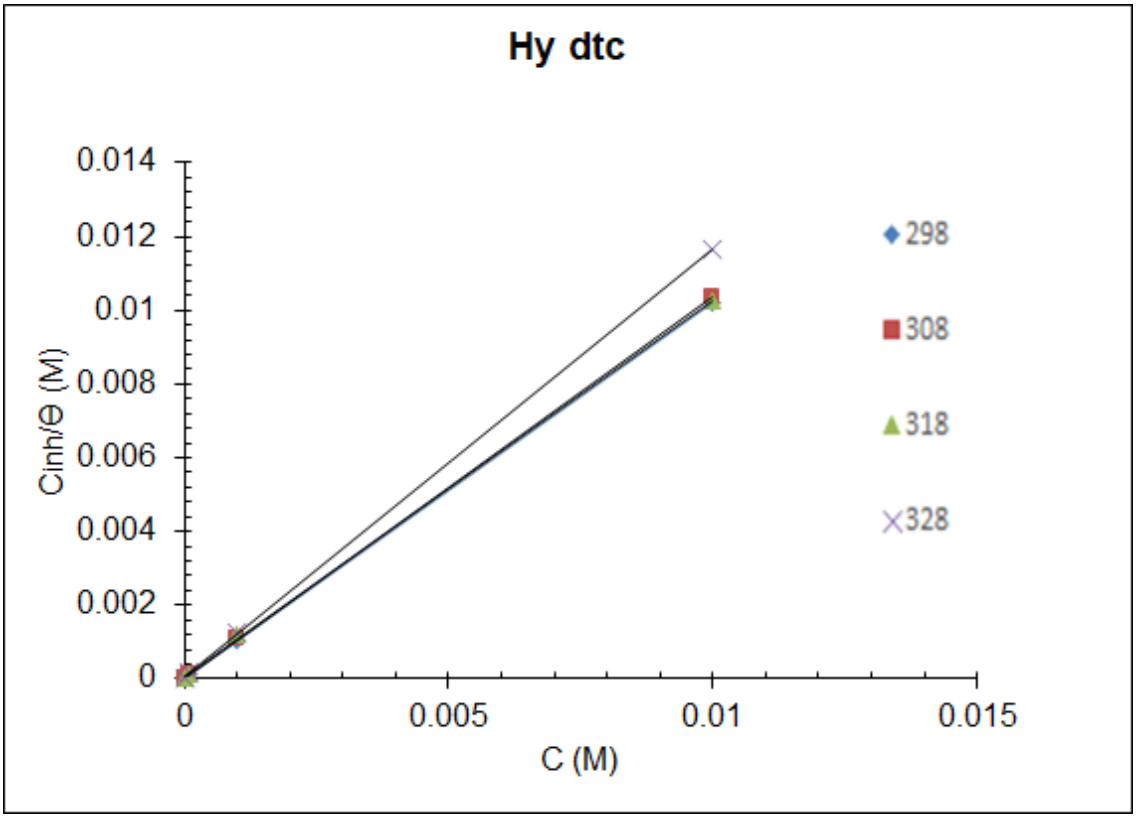

Fig.7. Adsorption behavior of (Hy-DTC) on the mild steel surface in 0.5 M H_2SO_4.

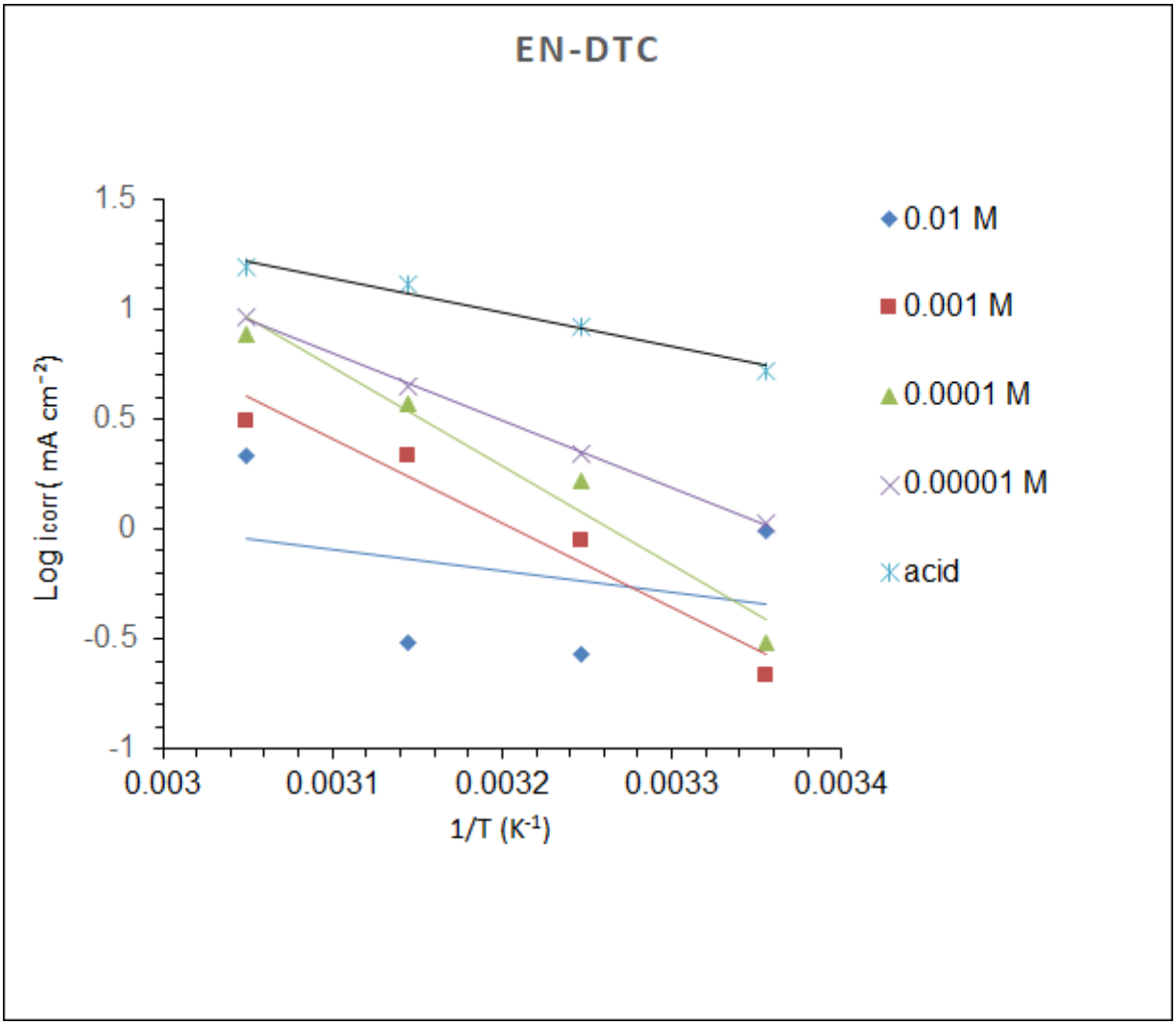

Fig.8. Plot of variation of Log I_{corr} vs 1/T for different concentrations of (En-DTC).

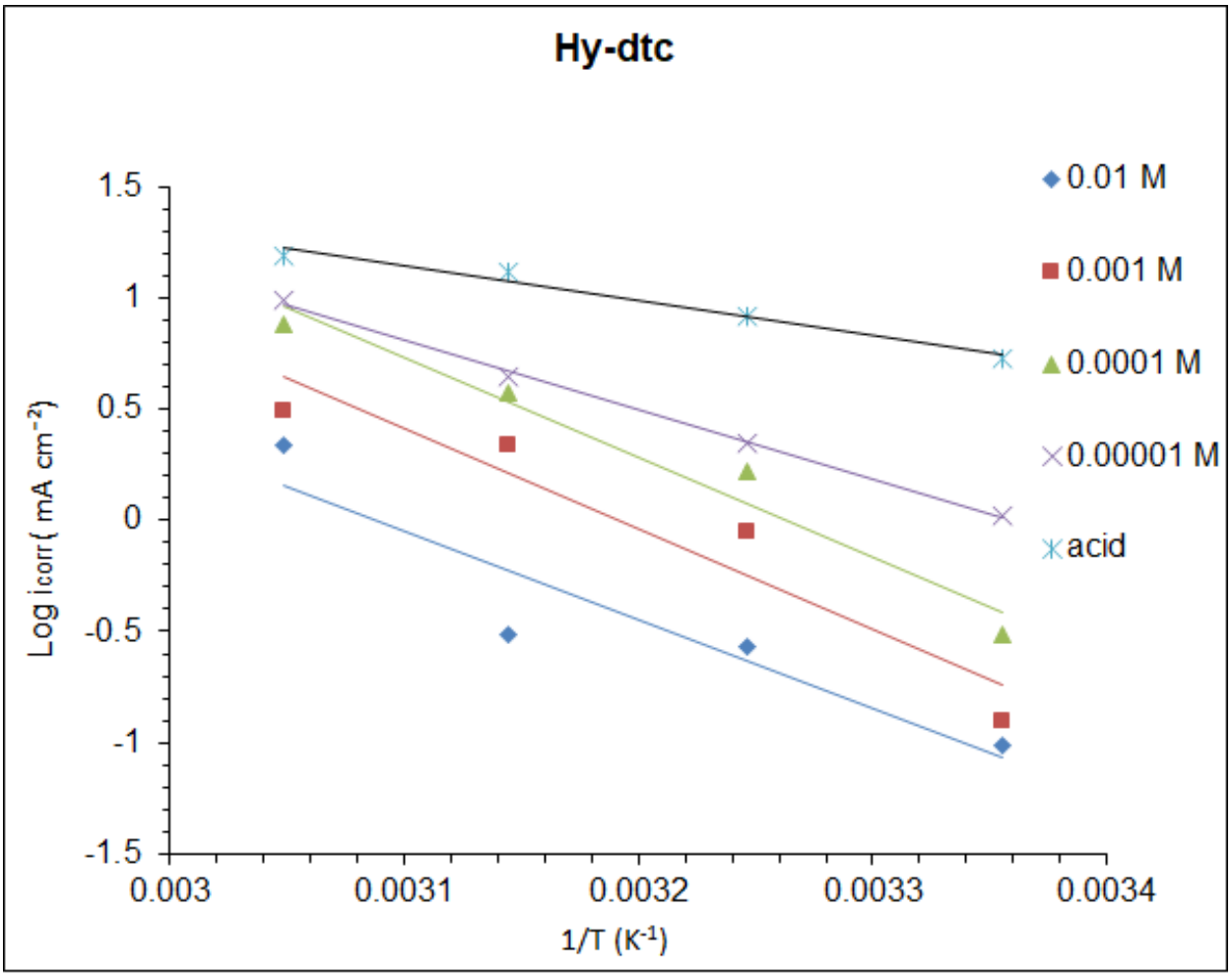

Fig.9. Plot of variation of Log I_{corr} vs 1/T for different concentration of (Hy-DTC).

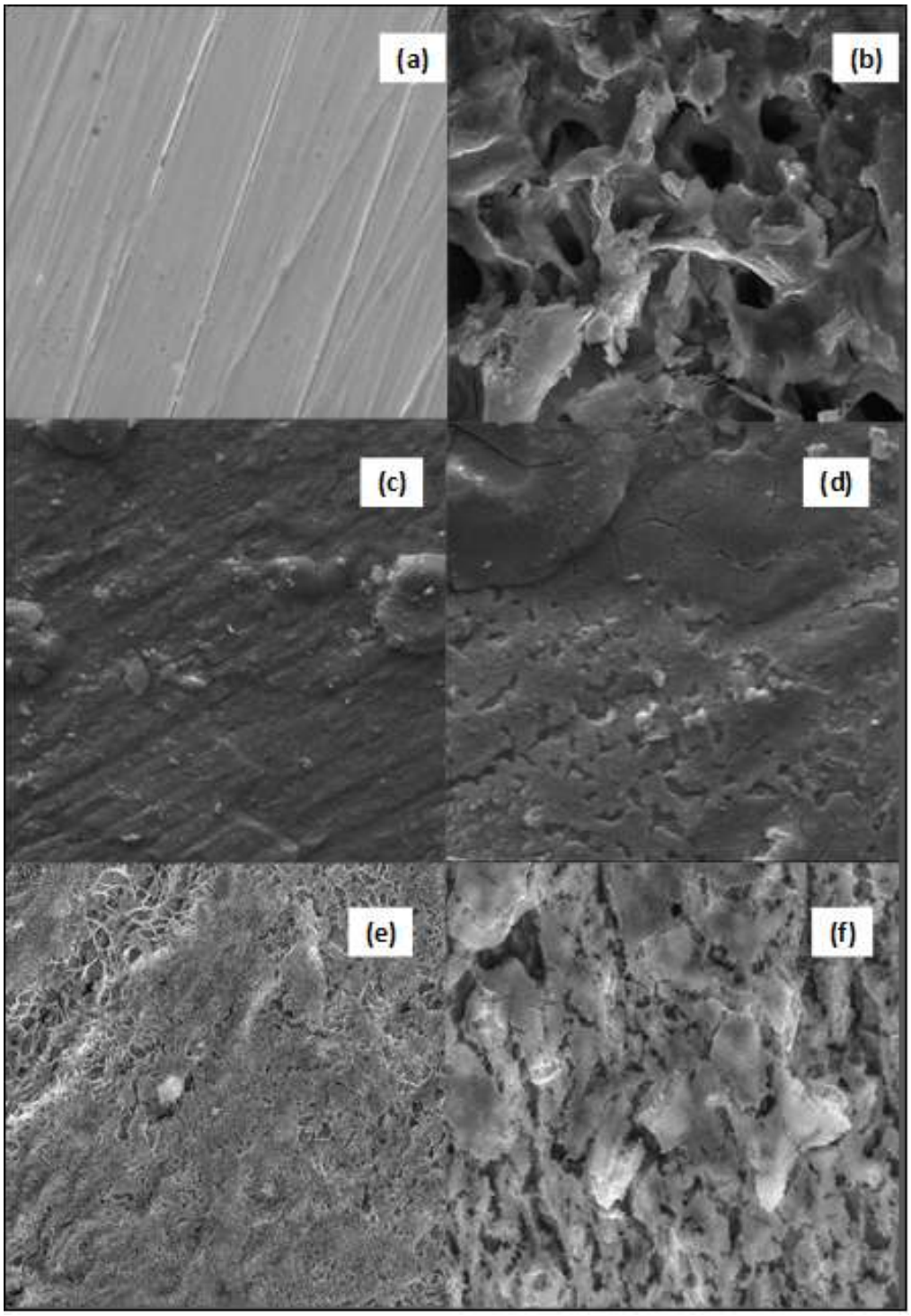

Fig.10. SEM images of surface of mild steel after immersion for 4 hrs in (b) 0.5 M H_2SO_4 and in the presence of (c) 10^{-2} M (d) 10^{-5} M En-DTC (e) 10^{-2} M (f) 10^{-5} M Hy-DTC [Magnification = 5000] at 298 K.

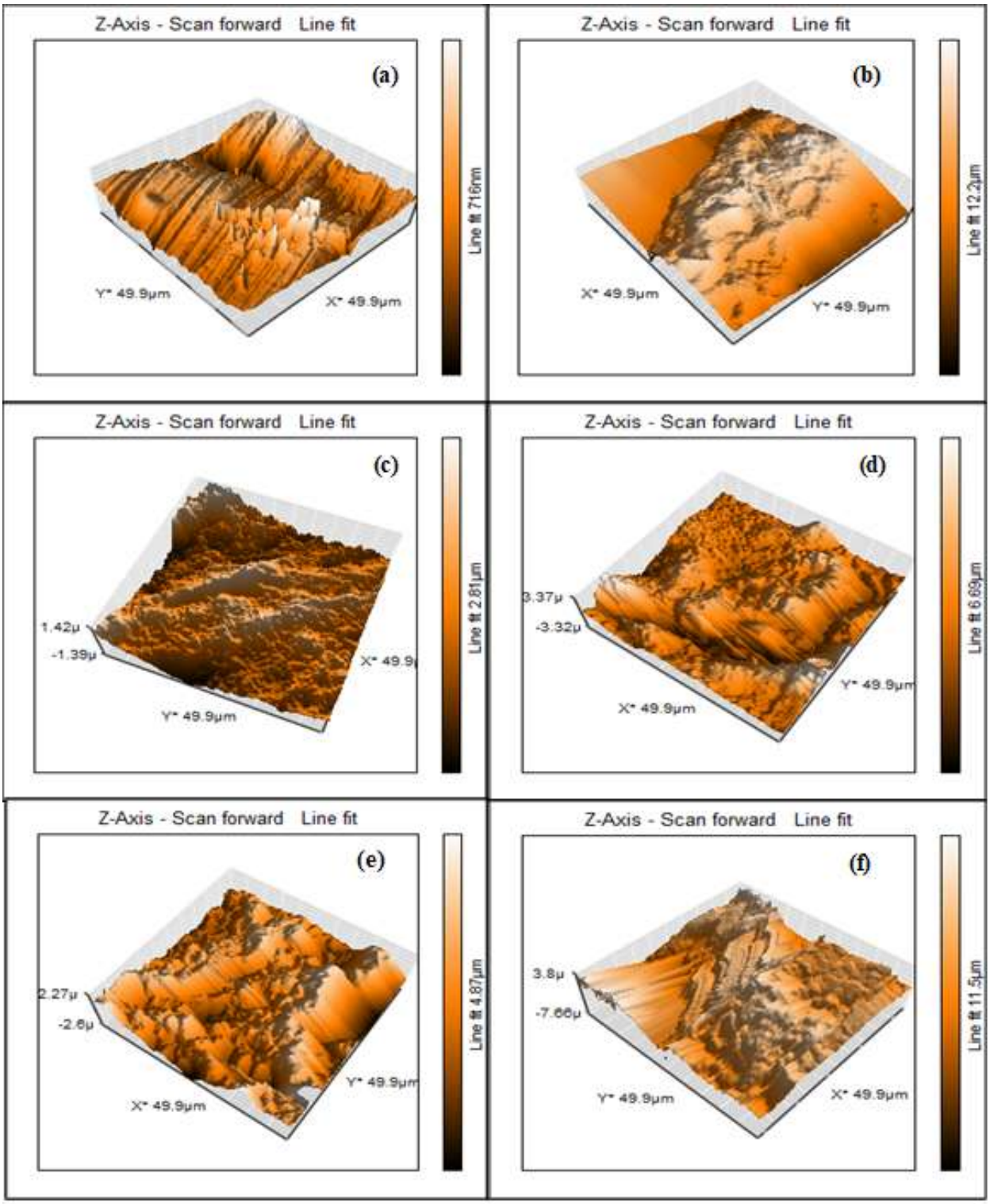

Fig.11. AFM Three-dimensional images of mild steel surfaces for (a) Mild Steel (b) 0.5 M H_2SO_4 (c) 10^{-2} M En-DTC (d) 10^{-5} M En-DTC (e) 10^{-2} M Hy-DTC (f) 10^{-5} M Hy-DT

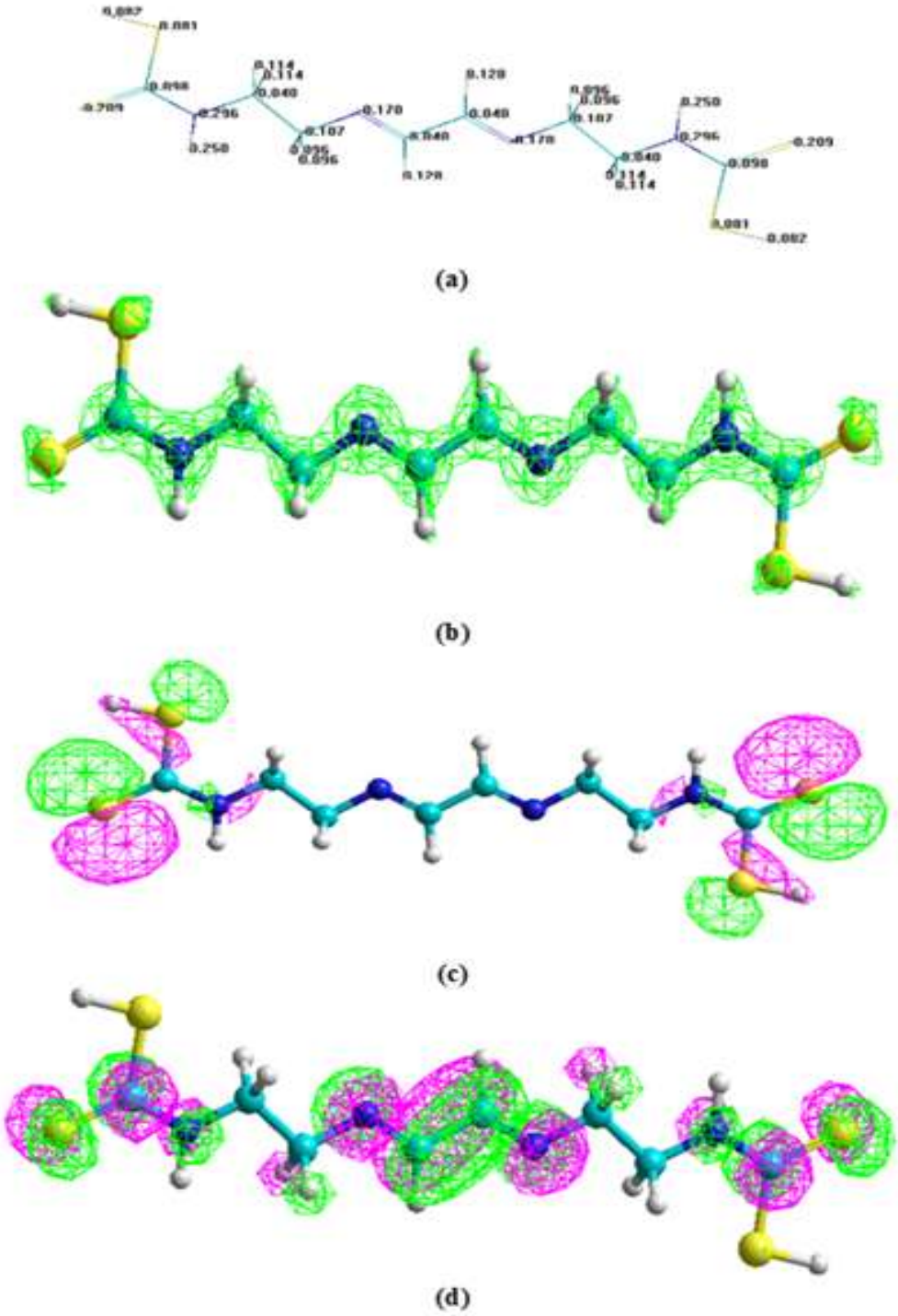

Fig.12. (a) Structure of En-DTC with Charge on Atoms (b) Molecular Orbital Plot for Total Charge Density (c) The Frontier Molecular Orbital Charge Density Distribution for HOMO and (d) The Frontier Molecular Orbital Charge Density Distribution for LUMO.

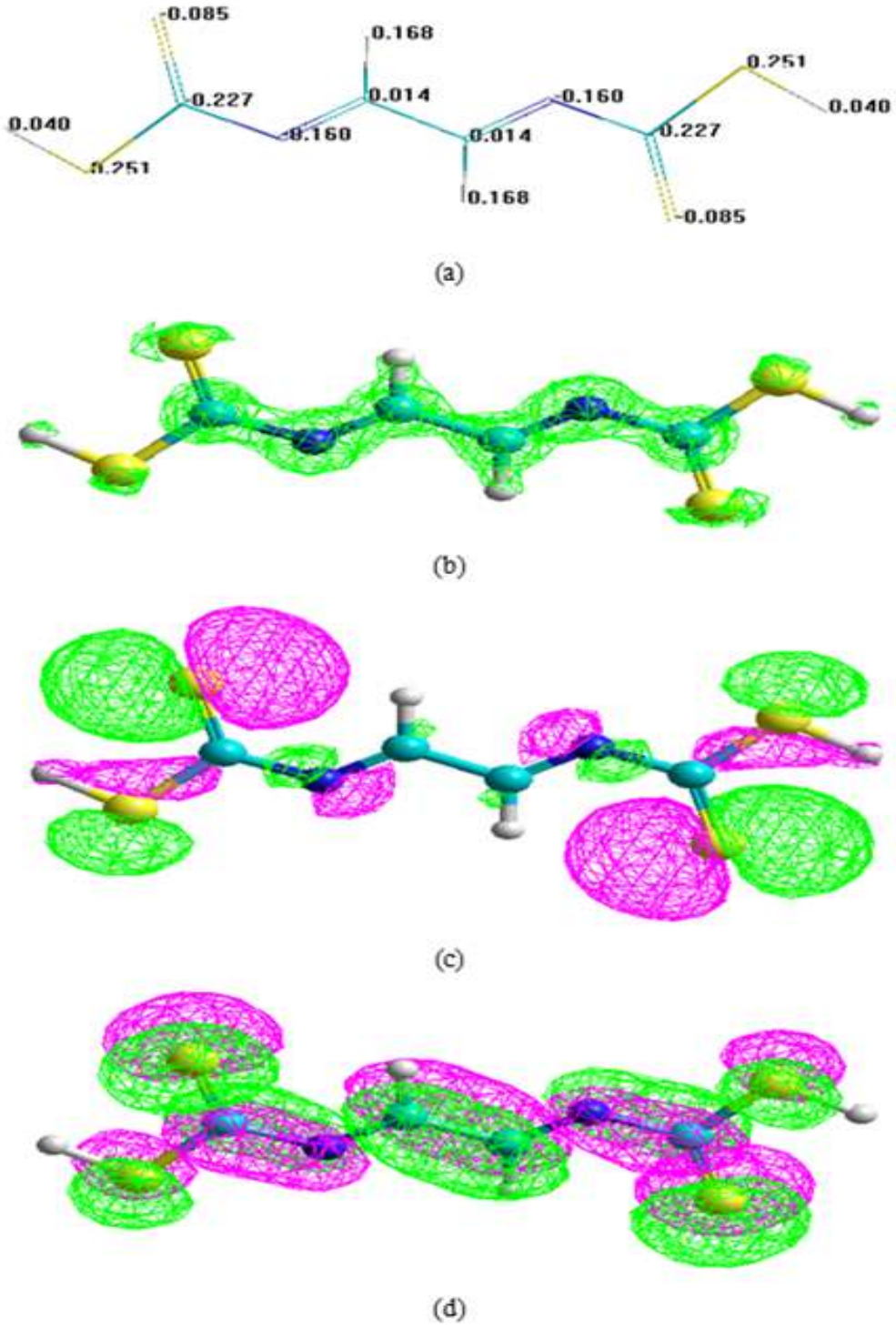

Fig.13. (a) Structure of Hy-DTC with Charge on Atoms (b) Molecular Orbital Plot for Total Charge Density (c) The Frontier Molecular Orbital Charge Density Distribution for HOMO and (d) The Frontier Molecular Orbital Charge Density Distribution for LUMO.

Table 1: Galvanostatic polarization parameters for the corrosion of mild steel in 0.5 M H_2SO_4 containing different concentration of (En-DTC).

Temp. (K)	Conc. (M)	$-E_{corr}$ (mV vs. SCE)	b_c (mV/decade)	b_a (mV/decade)	I_{corr} (mA cm^{-2})	I.E. (%)
298	10^{-2}	462	105	39	0.14	97
	10^{-3}	489	112	94	0.17	96
	10^{-4}	498	114	115	0.31	94
	10^{-5}	449	107	55	0.66	87
	0	477	155	124	5.29	0
308	10^{-2}	455	105	35	0.25	96
	10^{-3}	507	121	54	0.32	96
	10^{-4}	499	117	89	1.02	87
	10^{-5}	460	140	100	5.22	37
	0	514	154	155	8.33	0
318	10^{-2}	476	126	55	1.00	92
	10^{-3}	498	127	92	3.26	74
	10^{-4}	475	142	108	4.12	68
	10^{-5}	469	159	126	8.94	31
	0	480	175	164	13.01	0
328	10^{-2}	486	154	91	4.88	68
	10^{-3}	482	142	116	7.05	54
	10^{-4}	466	151	110	8.48	44
	10^{-5}	497	149	125	8.83	42
	0	480	177	170	15.43	0

Table 2: Galvanostatic polarization parameters for the corrosion of mild steel in 0.5 M H_2SO_4 containing different concentration of (Hy-DTC)

Temp. (K)	Conc. (M)	$-E_{corr}$ (mV vs. SCE)	b_c (mV/decade)	b_a (mV/decade)	I_{corr} (mA cm^{-2})	I.E. (%)
298	10^{-2}	487	104	63	0.09	98
	10^{-3}	446	94	62	0.12	97
	10^{-4}	458	103	72	0.30	94
	10^{-5}	470	114	86	1.06	79
	0	477	155	124	5.29	0
308	10^{-2}	461	95	72	0.26	96
	10^{-3}	464	112	79	0.88	89
	10^{-4}	474	123	77	1.64	80
	10^{-5}	485	136	95	2.21	73
	0	514	154	155	8.33	0
318	10^{-2}	485	115	120	0.30	97
	10^{-3}	467	123	78	2.17	83
	10^{-4}	491	148	112	3.73	71
	10^{-5}	478	157	121	4.44	65
	0	480	175	165	13.01	0
328	10^{-2}	482	136	137	2.16	85
	10^{-3}	486	141	177	3.12	79
	10^{-4}	481	182	140	7.64	50
	10^{-5}	474	175	165	9.17	40
	0	480	177	170	15.43	0

Table 3: Impedance parameters for the corrosion of mild steel in 0.5 M H_2SO_4 containing different concentration of (En-DTC and Hy-DTC)

Inhibitor	**C_{inh} (M)**	**R_{ct} (Ω cm^{-2})**	**f_{max} (Hz)**	**C_{dl} (μF cm^{-2})**	**I.E. (%)**
Blank	0	13.96	7.19	1584	-
En-DTC	10^{-5}	100.94	28.75	54.86	86
	10^{-4}	268.36	83.28	7.12	94
	10^{-3}	278.73	99.10	5.76	95
	10^{-2}	466.51	164.23	2.07	97
Hy-DTC	10^{-5}	120.34	45.10	29.33	88
	10^{-4}	187.94	64.03	13.23	92
	10^{-3}	394.62	115.92	3.48	96
	10^{-2}	560.46	167.91	1.69	97

Table 4: Thermodynamic parameters for the adsorption of En-DTC and Hy-DTC on MS 0.5 M H_2SO_4 solutions.

Inhibitor	**Temperature (K)**	**K_{ads} x 10^4 M^{-1}**	**$-\Delta G^{\circ}_{ads}$ (kJ mol^{-1})**	**$-\Delta H^{\circ}_{ads}$ (kJ mol^{-1})**	**$-\Delta S^{\circ}_{ads}$ (JK^{-1} mol^{-1})**
En-DTC	298	25	40.75	114.38	247.10
	308	10	39.77		
	318	1	34.97		
	328	0.5	34.18		
Hy-DTC	298	25	40.74	72.06	105.12
	308	2.5	36.21		
	318	1.42	35.90		
	328	1.66	37.45		

Table 5: Adsorption energies of En-DTC

Concentration (M)	**log A**	**R^2**	**E_a (kJ mol^{-1})**
10^{-2}	2.96	0.09	18.87
10^{-3}	12.24	0.94	73.11
10^{-4}	14.61	0.96	85.74
10^{-5}	10.24	0.99	58.38
H_2SO_4	5.97	0.97	29.82

Table 6: Adsorption energies of Hy-DTC

Concentration (M)	**log A**	**R^2**	**E_a (kJ mol^{-1})**
10^{-2}	12.28	0.87	76.19
10^{-3}	14.44	0.91	86.61
10^{-4}	14.61	0.96	85.74
10^{-5}	10.48	0.99	59.75
H_2SO_4	5.97	0.97	29.82

Table 7: Quantum chemical parameters for the corrosion of (En-DTC and Hy-DTC)

Inhibitor	**E (eV)**		**$\Delta E_{LUMO-HOMO}$ (eV)**	**Ionization energy (eV)**	**μ (D)**
	HOMO	**LUMO**			
En-DTC	-8.84	-0.59	8.25	8.84	1.73
Hy-DTC	-9.26	-2.43	6.83	9.26	1.88